Measurement of retinal blood flow in the rat by combining Doppler Fourier-domain optical coherence tomography with fundus imaging

René M. Werkmeister
Martin Vietauer
Corinna Knopf
Clemens Fürnsinn
Rainer A. Leitgeb
Herbert Reitsamer
Martin Gröschl
Gerhard Garhöfer
Walthard Vilser
Leopold Schmetterer

Measurement of retinal blood flow in the rat by combining Doppler Fourier-domain optical coherence tomography with fundus imaging

René M. Werkmeister,[a] Martin Vietauer,[a,b] Corinna Knopf,[a] Clemens Fürnsinn,[c] Rainer A. Leitgeb,[a] Herbert Reitsamer,[d] Martin Gröschl,[b] Gerhard Garhöfer,[e] Walthard Vilser,[f] and Leopold Schmetterer[a,e,*]
[a]Medical University of Vienna, Center for Medical Physics and Biomedical Engineering, Währinger Gürtel 18-20, 1090 Vienna, Austria
[b]Vienna University of Technology, Institute of Applied Physics, Wiedner Hauptstrasse 8-10/134, 1040 Vienna, Austria
[c]Medical University of Vienna, Department of Internal Medicine II, Währinger Gürtel 18-20, 1090 Vienna, Austria
[d]Paracelsus University, Department of Ophthalmology, Müllner Hauptstraße 48, 5020 Salzburg, Austria
[e]Medical University of Vienna, Department of Clinical Pharmacology, Währinger Gürtel 18-20, 1090 Vienna, Austria
[f]Imedos Systems UG, Am Nasstal 4, 07751 Jena, Germany

Abstract. A wide variety of ocular diseases are associated with abnormalities in ocular circulation. As such, there is considerable interest in techniques for quantifying retinal blood flow, among which Doppler optical coherence tomography (OCT) may be the most promising. We present an approach to measure retinal blood flow in the rat using a new optical system that combines the measurement of blood flow velocities via Doppler Fourier-domain optical coherence tomography and the measurement of vessel diameters using a fundus camera-based technique. Relying on fundus images for extraction of retinal vessel diameters instead of OCT images improves the reliability of the technique. The system was operated with an 841-nm superluminescent diode and a charge-coupled device camera that could be operated at a line rate of 20 kHz. We show that the system is capable of quantifying the response of 100% oxygen breathing on the retinal blood flow. In six rats, we observed a decrease in retinal vessel diameters of 13.2% and a decrease in retinal blood velocity of 42.6%, leading to a decrease in retinal blood flow of 56.7%. Furthermore, in four rats, the response of retinal blood flow during stimulation with diffuse flicker light was assessed. Retinal vessel diameter and blood velocity increased by 3.4% and 28.1%, respectively, leading to a relative increase in blood flow of 36.2%. The presented technique shows much promise to quantify early changes in retinal blood flow during provocation with various stimuli in rodent models of ocular diseases in rats. © The Authors. Published by SPIE under a Creative Commons Attribution 3.0 Unported License. Distribution or reproduction of this work in whole or in part requires full attribution of the original publication, including its DOI. [DOI: 10.1117/1.JBO.19.10.106008]

1 Introduction

Abnormalities in ocular blood flow have been connected with a variety of ocular diseases including diabetic retinopathy, age-related macular degeneration, and glaucoma.[1–5] However, quantification of retinal blood flow is difficult. Color Doppler imaging measures blood velocities in retrobulbar vessels, but no information on vessel diameters is available.[6] Laser Doppler flowmetry and speckle flowgraphy can be used to assess choroidal and optic nerve blood flow in relative units.[7,8] For several years, the only technique providing information about retinal blood flow was the combined measurement of retinal blood velocity via laser Doppler velocimetry (LDV) and of vessel diameters using fundus photographs.[9] By measuring retinal vessel diameters using the dynamic vessel analyzer (DVA) and retinal blood velocities using bi-directional LDV, however, it was shown that the range of retinal blood flow values in healthy humans is wide.[10] As such, it may be more attractive to study the response of the retinal vasculature to stimuli such as flicker light or 100% oxygen

breathing. Indeed, it has been shown that the hyperemic response to flicker stimulation[11,12] and the vasoconstrictor response to 100% oxygen breathing are compromised in early diabetic retinopathy.[13]

In the recent years, optical coherence tomography (OCT), a noninvasive high-resolution imaging technique that offers the possibility of performing *in vivo* optical "biopsy" of tissue structures, has become standard in the imaging of the anterior and posterior segments of the eye.[14] Doppler OCT, as a functional extension of OCT, allows the extraction of phase shifts in the backscattered light, thus the ability to gain information on movements in the probed tissue region.[11,12,15] Recently, several systems were realized aiming toward the quantification of retinal blood flow using Doppler OCT in humans.[16–20]

We set out to develop a novel system that is capable of measuring changes in retinal blood flow in the rat. The system uses the combination of Fourier-domain Doppler OCT for the extraction of retinal blood velocities and a fundus camera-based optical part of the system for the measurement of retinal vessel diameters. The capability of this system to quantify changes in retinal blood flow during 100% oxygen breathing and stimulation with diffuse luminance flicker was demonstrated *in vivo*.

---

*Address all correspondence to: Leopold Schmetterer, E-mail: leopold.schmetterer@meduniwien.ac.at

2 Methodology

### 2.1 Doppler Fourier-Domain-Optical Coherence Tomography

Blood flow velocity measurements were carried out via Doppler Fourier-domain OCT (FDOCT) operating in the near-infrared wavelength range. To measure blood flow velocities via FDOCT, the phase difference $\Delta\Phi(z)$ at the same point between adjacent A-line recordings after Fourier transform was calculated. Since one only has access to phase changes parallel to the incident probe beam direction, the tilting angle between the velocity vector under study and the probe beam, i.e., the Doppler angle, has to be taken into account. The flow velocity V is then given by

$$V(z) = \Delta\Phi(z) \frac{\lambda_0}{4\pi n\tau \cos\alpha}, \qquad (1)$$

where λ_0 is the central wavelength of the light source and τ is the time period between subsequent A-scans. n in Eq. (1) denotes the group refractive index of blood which was—as an average of values for 632.8 and 1080 nm[21]—estimated to be 1.37. The theoretic maximum accessible longitudinal velocity V_{max} is limited by the detection speed of the charge-coupled device (CCD) and can be obtained from Eq. (1); with a central wavelength of 841 nm and an A-scan rate of 20 kHz and assuming $\Delta\Phi_{max} = \pi$ and $\alpha = 0$, it amounts to 3 mm/s. However, since the measurements presented here were performed on the posterior pole of the eye on vessels around the optic nerve head (ONH)—with a distance of about one to two disk diameters from its rim—the incidence angle is much larger, in the range of 90 deg, and higher velocity values can be measured. V_{max} without any wrapping artifacts was—depending on the Doppler angle—in the range of 10 to 20 mm/s. Yet higher velocities can be measured by compensating for the wrapping artifacts as described in the next section. The minimum velocity is given by the phase noise $\Delta\Phi_{err}$ present in the system, and can—for a single-beam Doppler OCT system–calculated as $V_{min} = \lambda \cdot \Delta\Phi/(4\pi \cdot \tau)$.[22] However, this equation only holds true for a Doppler angle of zero degrees, which does not hold when measurements are performed in the posterior pole of the eye. With the phase noise of $\Delta\Phi_{err} = 0.18$ rad, measured when scanning was performed, we were able to assess velocities as low as 2.5 mm/s.

The optical setup of the measurement system is depicted in Fig. 1. As light source, a superluminescent diode (Superlum, Carrigtwohill, Cork, Ireland) with a central wavelength λ_0 of 841 nm and a full width at half maximum bandwidth $\Delta\lambda$ of 50 nm was used. This resulted in an axial resolution in air of 6 μm. A beamsplitter with a splitting ratio of 50:50 divided the light coming from the source into the sample and reference arms. The free-space pathway of the reference arm contained a variable neutral density (ND) filter and a pair of prisms for balancing dispersion due to the optic components in the sample arm. In the sample arm, light was collimated by means of a fiber collimator, passed two galvanometric mirrors (GVS002; Thorlabs GmbH, Dachau/Munich, Germany) for scanning in two dimensions, and illuminated the eye via the lenses L1 and L2, where L2 is the ophthalmic lens of the retinal vessel analyzer. The interference spectrum returning from the interferometer was directed onto a 50×50 mm transmission grating with $L = 1200$ lines per mm (Wasatch Photonics, Logan, Utah) using a collimator with a focal length $f = 100$ mm (OZ Optics, Ottawa, Canada). The dispersed light emerging from the transmissive grating was imaged onto a CCD camera (Atmel AVIIVA M2 CL2014, Aviva, Essex, UK) with a pixel size of 14×14 μm by means of an achromatic lens ($f = 100$ mm).
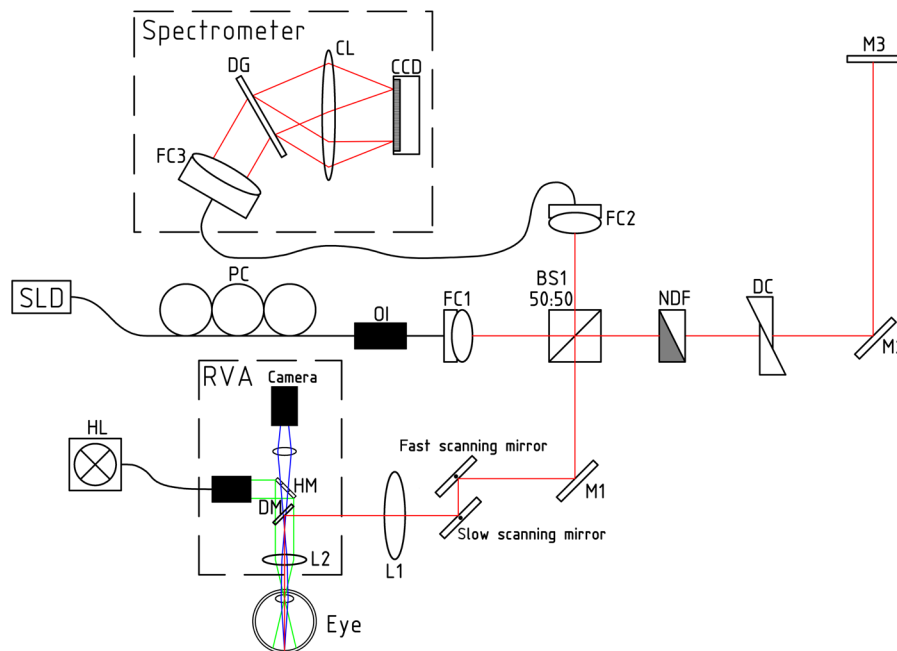
Fig. 1 Schematic representation of the Doppler optical coherence tomography (OCT) system and coupling to the rat fundus camera. SLD, superluminescent diode; PC, polarization controller; OI, optical isolator; FC, fiber collimator; BS, beam splitter cube; NDF, neutral density filter; DC, dispersion compensation; M_i, Mirror; DM, dichroic mirror; L1, L2, lens; HL, halogen lamp; DG, diffraction grating; CL, camera lens; HM, hole mirror.

The transversal resolution, given by the diameter of the collimated probe beam at the cornea and the focal length of the rat eye, is approximately 11 μm. The oversampling factor (OF) of the phase tomograms is defined as $OF = w \cdot N/d$, where w is the spot size, N is the number of sampling points, and d is the geometric width of the tomogram.[23] With the above given spot size, $N = 1000$ sampling points for *in vivo* measurements, and a scan width of 1.1 mm, one obtains an OF of 10. The power of the probe beam incident on the rats' corneas was measured to be 650 μW. The time period τ between two subsequent CCD recordings (A-scan) was set to 50 μs, which—with a lateral tomogram dimension of 1000 A-lines for *in vivo* measurements—gives a frame rate of 20 s^{-1}.

As a first OCT postprocessing step, the tomograms were corrected for sample motion using a histogram-based method.[24,25] Vessel positions within the tomogram were detected via convolution of the phase image with an elliptical template.

Phase values calculated via Fourier transform lie in the range $[+\pi, -\pi]$. However, in larger arteries and veins, where flow velocities are quite high, phase values can exceed this unambiguous range, leading to phase wrapping artifacts. These artifacts result in a seeming reversal of the flow in the vessel center. By determining the "true" flow direction close to the vessel wall and adding or subtracting 2π to/from the corresponding phase value, these regions were unwrapped.

Further, several postprocessing steps were performed: missing Doppler data points that occur as a result of fringe washout, particularly in the center of the vessel, were reconstructed by applying a parabolic fit to the available data points.[18] In addition, resampling of the vessel data using bi-cubic interpolation was employed for achieving equal lateral and axial resolution. For the calculation of the average phase within the vessel cross-sectional area, the circular approach introduced by Szkulmowska et al.[26] was used. Briefly, the method uses the fact that the phase differences $\Delta\Phi$ are randomly distributed around the actual values. When phase averaging is performed in the angular domain, this leads to an underestimation of the mean phase difference, especially at high velocities close to the $\pm\pi$ limit. Therefore, the phase values are transformed into a complex representation and the averaging is performed by calculating the argument of the complex sum. The average flow velocity V_{avg} was computed over a minimum of four to five pulse periods.

Retinal vessel diameters were assessed by means of a fundus camera-based DVA system (DVA rodent, Imedos, Jena, Germany) that does not require contact with the eye, and does not influence the retinal microcirculation. Recently, the application of the DVA technique in rodents has been described

for such a system using a retinal camera adapted to the rat eye, an illumination unit and the DVA software platform also used for the human system.[27] The DVA system used for the current experiments allows for the online measurements of retinal arterial and venous diameters with excellent reproducibility.[8] This is because the optical system is adapted specifically to the optical properties of the rat eye with its specific illumination and imaging requirements. The measurement resolution of the system is, due to the higher magnification as compared to the human system and the applied algorithms for vessel boundary detection, up to 0.1 μm. This allows for assessment of vessel diameters in retinal vessels down 30 μm in both pigmented and nonpigmented animals.

The Doppler OCT and the DVA rodent were coupled by means of a dichroic mirror DM, placed between the ophthalmic lens L2 and the hole mirror HM of the DVA system. This dichroic mirror lets the DVA's light in the visible wavelength range pass unimpeded while redirecting the OCT probe beam (near-infrared wavelength range) into the fundus cameras' optical path.

2.2 Animal Preparation

The study followed the association for research in vision and ophthalmology statement for the use of animals in ophthalmic and vision research and was approved by the ethical committee of the Medical University of Vienna. Six male Sprague–Dawley rats with a body weight of 400 to 600 g were used in the experiments. Anesthesia was induced with a mixture of 100 mg/kg ketamine and 5 mg/kg xylazine, injected intraperitoneally. The rodents were intubated and, during the surgical procedure, ventilated with O_2, air and 2% isofluran. Via a venous access, the animals were given a bolus of 20 mg/kg gallamine triethiodide (Sigma Aldrich, Vienna, Austria; G8134) followed by a continuous intravenous infusion of 50 mg/kg/h ketamine, 0.05 mg/kg/h fentanyl, and 20 mg/kg/h gallamine triethiodide (Sigma Aldrich; G8134). To maintain good imaging properties, the eyes of the rats were continuously moistened with hyaluronic acid containing eye drops (Hylo-Comod® 1 mg/ml sodium hylauronat; Ursapharm, Saarbrücken, Germany). In all animals, only the right eye was used for measurements. After the experiments, the rodents were euthanized via cervical dislocation and exsanguination.

2.3 Measurement Protocol

All results presented in this paper were gained from blood flow velocity and vessel diameter measurements in large retinal
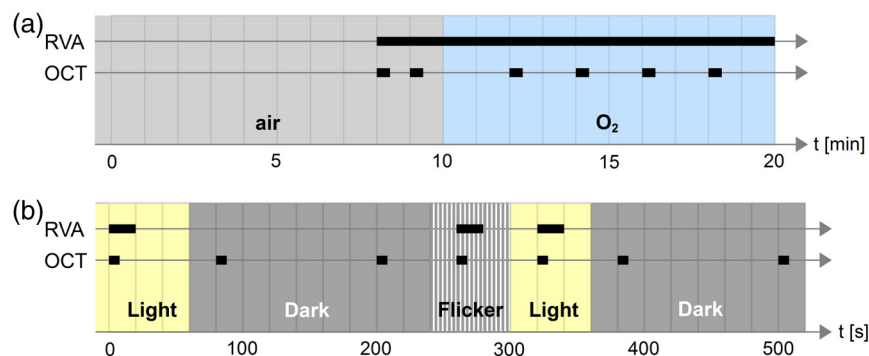
Fig. 2 Measurement protocols: timelines for (a) hyperoxia and (b) flicker experiments.

vessels. The measurement protocol for the hyperoxia experiments is shown in Fig. 2(a): the rodents were narcotized and ventilated with ambient air for 10 min. Thereafter, 100% oxygen was administered for another 10 min. In each animal, one major retinal vein was selected and measurements were carried out at a distance of about one disk diameter from the ONH. Starting at 8 min of the air breathing phase, the vessel diameters were continuously recorded during the whole session. Blood flow velocity measurements were performed at 8 and 9 min of the air breathing phase (baseline) and at 2, 4, 6, 8, 9, and 10 min of the oxygen breathing phase. The OCT recordings lasted 14 s to allow averaging of the phase data and calculating the mean blood flow velocities.

For all light stimulus experiments, the ambient light was dimmed to avoid corruption of the measured effects. Diffuse flicker illumination was applied at a frequency of 12 Hz via the fundus illumination path of the DVA. Each measurement session started with fundus illumination on: both the vessel diameter (via DVA) and blood flow velocity (via Doppler OCT) were measured at time point zero. After 60 s, the fundus illumination was switched off and Doppler OCT measurements were performed at time points 80 and 200 s. The dark phase lasted 3 min. Thereafter, the diffuse flicker phase started and lasted 60 s. Again, both vessel diameter and blood flow velocity of a single retinal vessel were measured at time point 260 s. At time point 300 s, the flicker illumination was switched off and the rat's fundus was illuminated via the DVA's halogen lamp for 60 s. At time point 320 seconds, further Doppler OCT and DVA measurements were performed before switching off the fundus illumination and repeatedly measuring flow velocities at time points 380 and 500 s. The timeline for the conducted measurements is depicted in Fig. 2(b).

2.4 Statistical Analysis

Descriptive analysis was used to characterize the data. Changes over baseline were analyzed using a repeated measures ANOVA model. All data are presented as means $\pm$ SD. A p-value <0.05 was considered the level of significance. Statistical analysis was carried out using CSS Statistica for Windows® (Statsoft Inc., Version 6.0, Tulsa, California).

3 Results

Two phase tomograms as obtained from Doppler measurements on a rat's retina are shown in Fig. 3. In Fig. 3(a), the phase tomogram including a vein with a diameter of approximately 50 μm or 100 pixels under basal conditions is shown. The measured vessel clearly shows a wrapping artifact in the center. The phase profile within the vessel after unwrapping is depicted in Fig. 3(c) and is close to parabolic. In Fig. 3(b), the phase tomogram of the same vein is shown during 100% oxygen breathing. In the phase tomogram, the vasoconstriction, indicated by a smaller vessel lumen, and the reduction in blood velocity, cognizable by the disappearance of the wrapping artifact, are clearly visible. This is also evident from the phase profile presented in Fig. 3(d), which, despite the largely reduced blood velocity, remains almost parabolic and shows a decrease of the vessel diameter by about 15 pixels.

In Fig. 4, the time courses of vessel diameter (black line), relative blood flow velocity (red squares), and relative blood flow (blue squares) in a single retinal vessel during breathing of 100% oxygen are depicted. As seen, the vessel diameter starts to decrease soon after the beginning of the 100% oxygen breathing. At approximately 360 s, full vasoconstriction is obtained and, thereafter, the vessel diameter remains constant. The
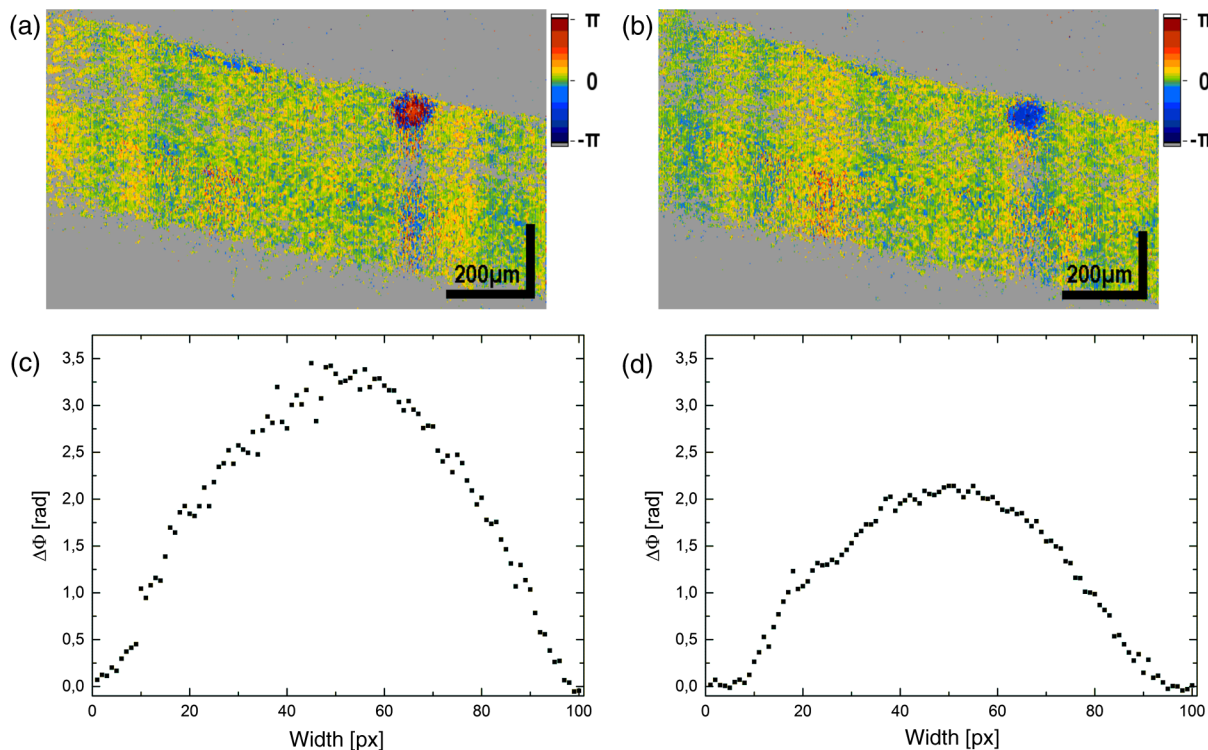
Fig. 3 Phase tomograms including a retinal vein and extracted phase profile (a), (c) under baseline conditions and (b), (d) during breathing 100% oxygen. The extracted phase is directly proportional to the blood velocity.
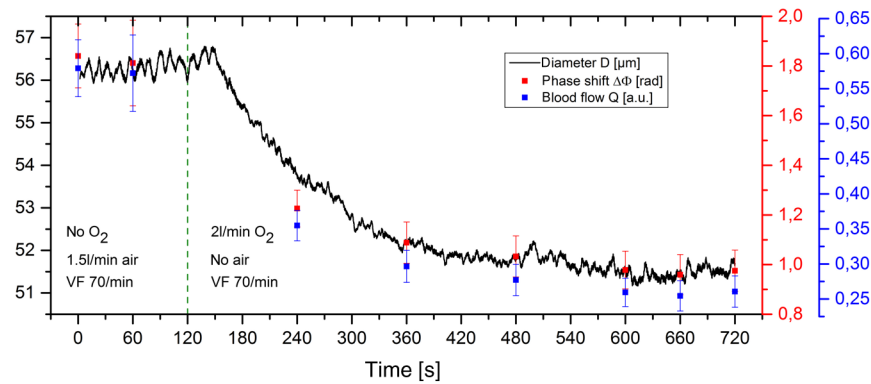
Fig. 4 Time courses of retinal venous diameter D, phase shift (ΔΦ) and blood flow (Q) during 100% oxygen breathing. Red symbols indicate the phase shift, which is proportional to the mean blood flow velocity. VF, ventilator frequency. Dashed lines indicate the change of breathing gases.

pronounced reduction in retinal blood velocity and retinal blood flow is already visible 120 s after the start of oxygen breathing (i.e., 240 s after the beginning of the experiment). In agreement with the diameter data, almost stable conditions are achieved at 360 s after the start of the experiment. Both velocity and flow decrease almost in parallel because the reduction in blood velocity is more pronounced than the reduction in vessel diameter or vessel cross-sectional area.

The average data as obtained in the six rats are presented in Fig. 5. At 600 s after the start of the oxygen breathing, we observed a reduction of $42.6 \pm 5.2\%$, $13.2 \pm 5.2\%$, and $56.7 \pm 7.4\%$ in blood flow velocity, vessel diameter and blood flow, respectively ($p < 0.001$ versus baseline each).
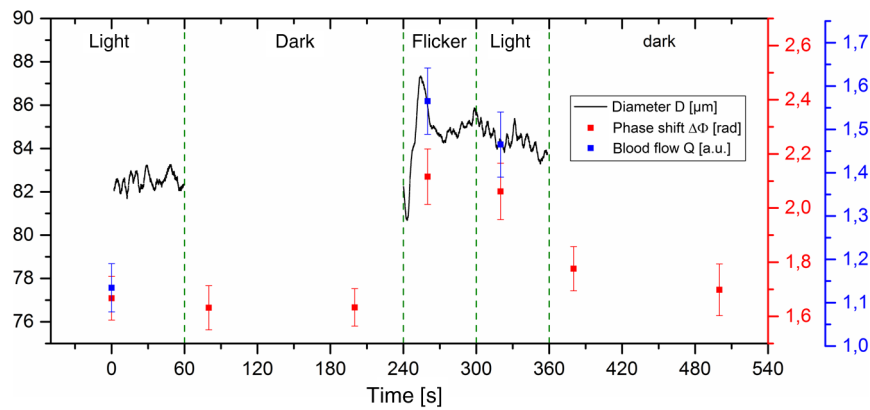
The time courses of the vessel diameter, blood flow velocity, and blood flow in one rat during stimulation with diffuse flicker light are presented in Fig. 6. During the dark periods, no measurements of vessel diameters via DVA were carried out. Typically, a short-lasting increase in vessel diameters was immediately seen after changing from dark to flicker

stimulation, but the vessel diameter returned almost to its baseline value thereafter. In contrast, Doppler OCT data could be also obtained during the dark periods. As seen, the retinal blood velocity was typically slightly lower in the dark as compared to the light conditions. Since no information on the vessel diameter was available, no flow values were calculated during darkness. Stimulation with flicker light increased both blood velocity and blood flow. During lightening conditions, the retinal blood velocity stayed elevated as compared to darkness.

In Fig. 7, the average increase in retinal blood velocity, vessel diameter, and blood flow in all four rats during the experiments is shown. The transition from light to dark did not change the blood velocity [Fig. 7(a)]. During flicker stimulation, on the other hand, a pronounced increase in blood velocity of 28.1% was observed ($p < 0.001$ versus baseline). When the diffuse luminance flicker was turned off, the blood velocity decreased slightly but was still higher than at baseline ($p < 0.001$). When the light was turned off, however, the retinal blood velocity returned to baseline again.
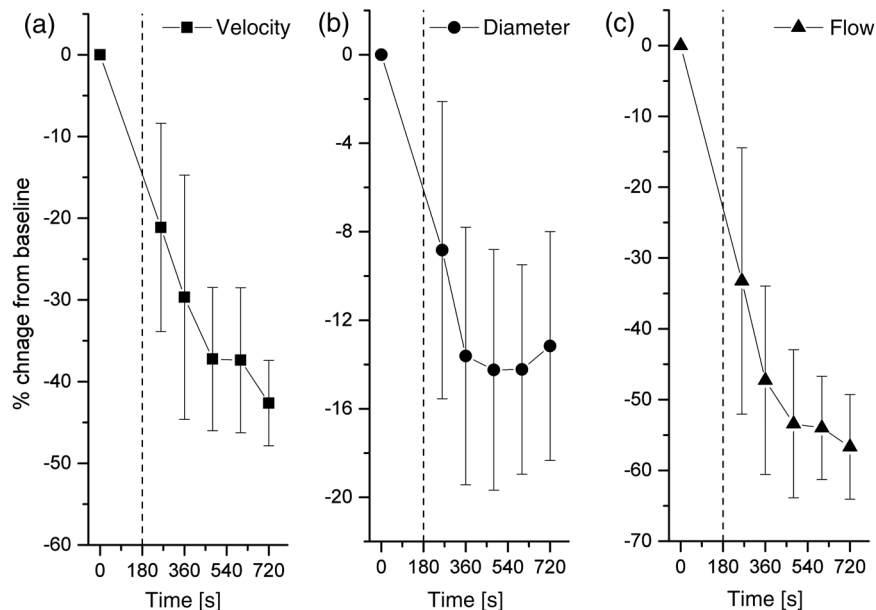
Fig. 5 Time courses of the relative change in (a) blood flow velocity, (b) venous diameter and (c) blood flow during 100% oxygen breathing ($n = 6$). Data are presented as means ± SD. The vertical line indicates the onset of 100% oxygen as breathing gas.

Fig. 6 Time courses of retinal venous diameter D, phase shift (ΔΦ) and blood flow (Q) during flicker stimulation. Red symbols indicate the time course of the phase shift, which is proportional to the blood flow velocity. During the periods in darkness no flow values are available, because vessel diameter was not measured.
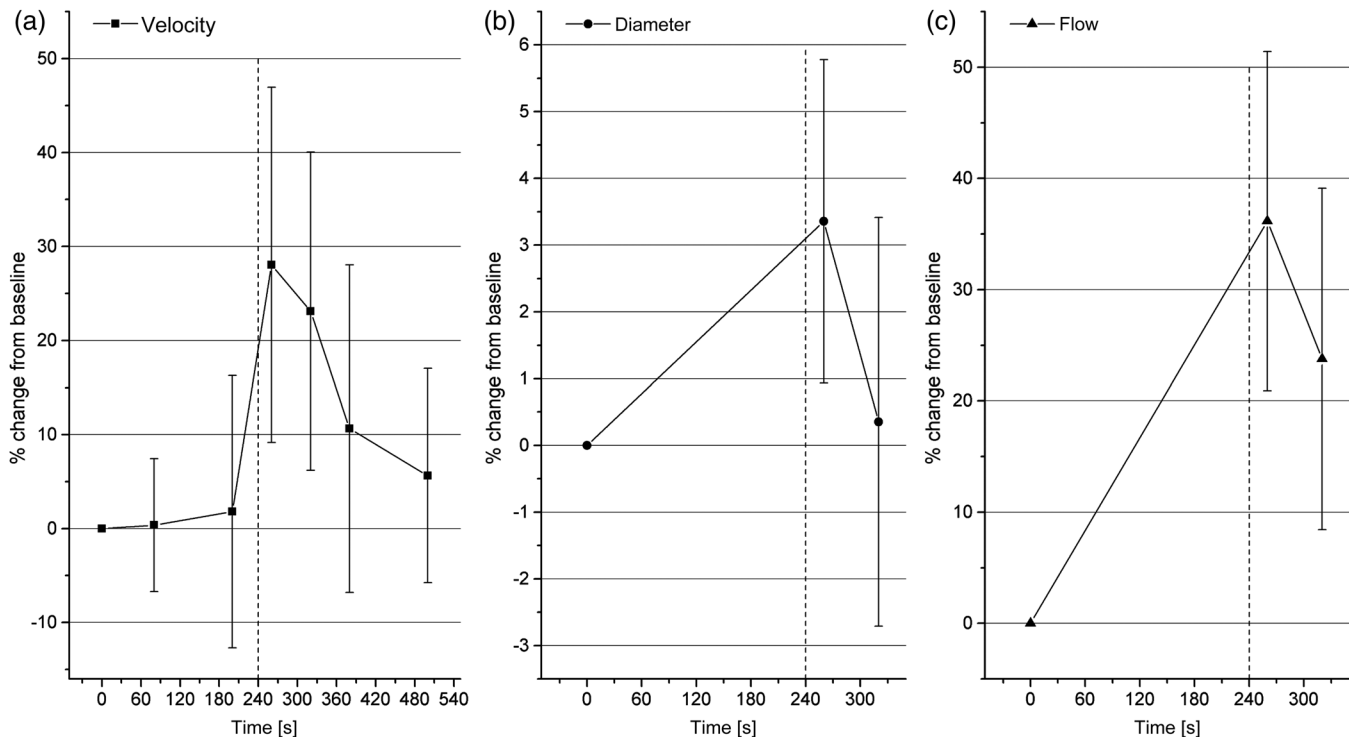
Fig. 7 Time courses of the relative change in (a) blood flow velocity, (b) vessel diameter and (c) blood flow during flicker stimulation ($n = 4$). Data are presented as means $\pm$ SD. Dashed lines indicate the onset of the flicker stimulus.

Figures 7(b) and 7(c) show the effect of flicker stimulation on retinal vessel diameter and retinal blood flow. Retinal vessel diameters slightly increased by 3.6% during flicker stimulation ($p < 0.05$ versus baseline) and returned to the baseline value thereafter. The retinal blood flow showed a strong increase (36.2%, $p < 0.001$ versus baseline) during flicker stimulation and stayed elevated after cessation.

4 Discussion

So far, no gold standard technique for the measurement of ocular blood flow has been realized.[6,19,28–30] Doppler OCT is a promising approach for measuring retinal blood flow. If absolute blood flow is to be measured, the angle ambiguity of the Doppler techniques has to be resolved. In humans, several techniques were realized to quantify retinal perfusion.[7,16,18,20,25,31–36] In rats, a technique was proposed to measure the axial blood velocity in an en-face plane using raster scanning in a very small area around the central retinal artery. The retinal blood flow was calculated by integrating over the vessel area.[20] For measurements of pulsatile total flow, very high acquisition speeds with axial scan rates in the range of several 100 kHz are necessary. In addition, transverse sampling density has to be sacrificed. Alternatively, gated acquisition can be applied to observe pulsatile retinal flow.[36] Other investigators used a

volumetric scanning protocol that asynchronously samples a single vessel with respect to the heartbeat, thus determining the averaged total blood flow.[37]

However, to which degree it is useful to study total retinal blood flow in the rat is unclear. In humans, total retinal blood flow shows a wide range in healthy subjects[10] and it is doubtful whether absolute blood flow measurements can be used for risk stratification in ocular disease. In rats, this is even more doubtful given the potential influence of anesthesia and the selected blood pressure value. As such, we focused on relative changes in retinal blood flow. One characteristic of our system is that it is coupled to a fundus camera allowing for the high-precision extraction of retinal vessel diameters from the fundus image, which is considered the gold standard technique for measuring retinal vessel width.[38] This is a critical issue, because the diameter of the vessels enters into the calculation of blood flow with the second order. Most other approaches determine the diameter from the OCT amplitude or phase images. The former method is difficult because of light scattering and absorption in retinal vessels, which often makes it complicated to identify the rear vessel wall. The latter is hampered by the phase noise and the lower limit of detectable velocity, which may lead to a velocity-dependent underestimation of the vessel width. However, both techniques are limited by the longitudinal resolution of OCT systems, which is usually in the range of 5 to 7 μm.

In the present study, we used hyperoxia as a stimulus, which induces pronounced vasoconstriction. A variety of techniques were previously used to characterize the retinal blood flow response to 100% oxygen breathing including magnetic resonance imaging[39] and scanning laser Doppler flowmetry.[40] These earlier studies reported a reduction in retinal blood flow of 25% and 24.5%, respectively. Our data show a reduction of 50 to 60% in retinal blood flow, which is closer to the values obtained in humans.[41–46] Studying the response of retinal blood flow to hyperoxia is interesting, because it has been shown to be disturbed early in diabetes.[47] However, the mechanisms which lead to this reduced vasoconstrictor response to hyperoxia are poorly understood.[48,49]

In contrast to hyperoxia, flicker light increases retinal blood flow due to a mechanism called neurovascular coupling. Increased neural activity as induced by light stimulation leads to an increased metabolic demand and to hyperemia of the retina and the ONH.[50–52] Several techniques were used to assess the retinal blood flow response to flicker stimulation including laser speckle flowgraphy,[53–55] fluorescent microspheres,[8] the measurement of retinal vessel diameters,[56] and Doppler OCT.[57] Our results indicate that most of the increase in retinal blood flow is due to the increase in blood velocity, whereas retinal vessel diameters showed only minor changes. This is in good agreement with human data indicating that most of the vasodilator response occurs in the microvasculature.[58] A reduction in the retinal response to flicker stimulation can be seen in diabetic patients before any change in pattern electro-retinography becomes evident.[59] In diabetic rats, the abnormal retinal flicker response can be normalized by inhibition of inducible nitric oxide synthase.[56]

In conclusion, we presented a method for measuring relative changes in retinal blood flow by combining the Doppler OCT technique with fundus camera-based measurement of retinal vessel diameters. The response to systemic hyperoxia and visual stimulation with flicker light was studied with this system. The technique has considerable potential in characterizing vascular abnormalities in animal models of retinal disease including diabetes.

References

1. B. Pemp and L. Schmetterer, "Ocular blood flow in diabetes and age-related macular degeneration," *Can. J. Ophthalmol.* **43**(3), 295–301 (2008).
2. J. Flammer and M. Mozaffarieh, "Autoregulation, a balancing act between supply and demand," *Can. J. Ophthalmol.* **43**(3), 317–321 (2008).
3. E. Mendrinos et al., "Lactate-induced retinal arteriolar vasodilation implicates neuronal nitric oxide synthesis in minipigs," *Invest. Ophthalmol. Vis. Sci.* **49**(11), 5060–5066 (2008).
4. D. Schmidl, G. Garhofer, and L. Schmetterer, "The complex interaction between ocular perfusion pressure and ocular blood flow: relevance for glaucoma," *Exp. Eye Res.* **93**(2), 141–155 (2011).
5. A. P. Cherecheanu et al., "Ocular perfusion pressure and ocular blood flow in glaucoma," *Curr. Opin. Pharmacol.* **13**(1), 36–42 (2013).
6. I. Stalmans et al., "Use of colour Doppler imaging in ocular blood flow research," *Acta Ophthalmol.* **89**(8), e609–e630 (2011).
7. C. Blatter et al., "Dove prism based rotating dual beam bidirectional Doppler OCT," *Biomed. Opt. Express* **4**(7), 1188–1203 (2013).
8. Y. Y. Shih et al., "Quantitative retinal and choroidal blood flow during light, dark adaptation and flicker light stimulation in rats using fluorescent microspheres," *Curr. Eye Res.* **38**(2), 292–298 (2013).
9. C. E. Riva et al., "Blood velocity and volumetric flow rate in human retinal vessels," *Invest. Ophthalmol. Vis. Sci.* **26**(8), 1124–1132 (1985).
10. G. Garhofer et al., "Retinal blood flow in healthy young subjects," *Invest. Ophthalmol. Vis. Sci.* **53**(2), 698–703 (2012).
11. B. White et al., "In vivo dynamic human retinal blood flow imaging using ultra-high-speed spectral domain optical coherence tomography," *Opt. Express* **11**(25), 3490–3497 (2003).
12. R. A. Leitgeb et al., "Real-time measurement of in vitro flow by Fourier-domain color Doppler optical coherence tomography," *Opt. Lett.* **29**(2), 171–173 (2004).
13. J. E. Grunwald et al., "Effect of pure O2-breathing on retinal blood flow in normals and in patients with background diabetic retinopathy," *Curr. Eye Res.* **3**(1), 239–241 (1984).
14. W. Drexler and J. G. Fujimoto, "State-of-the-art retinal optical coherence tomography," *Prog. Retin. Eye Res.* **27**(1), 45–88 (2008).
15. R. Leitgeb et al., "Real-time assessment of retinal blood flow with ultrafast acquisition by color Doppler Fourier domain optical coherence tomography," *Opt. Express* **11**(23), 3116–3121 (2003).
16. R. M. Werkmeister et al., "Bidirectional Doppler Fourier-domain optical coherence tomography for measurement of absolute flow velocities in human retinal vessels," *Opt. Lett.* **33**(24), 2967–2969 (2008).
17. Y. Wang et al., "Measurement of total blood flow in the normal human retina using Doppler Fourier-domain optical coherence tomography," *Br. J. Ophthalmol.* **93**(5), 634–637 (2009).
18. A. S. Singh et al., "Stable absolute flow estimation with Doppler OCT based on virtual circumpapillary scans," *Biomed. Opt. Express* **1**(4), 1047–1058 (2010).
19. C. J. Pournaras and C. E. Riva, "Retinal blood flow evaluation," *Ophthalmologica* **229**(2), 61–74 (2013).
20. W. Choi et al., "Measurement of pulsatile total blood flow in the human and rat retina with ultrahigh speed spectral/Fourier domain OCT," *Biomed. Opt. Express* **3**(5), 1047–1061 (2012).
21. V. V. Tuchin, *Optical Clearing of Tissue and Blood*, SPIE Press, Bellingham, Washington (2005).

22. T. Schmoll, C. Kolbitsch, and R. A. Leitgeb, "Ultra-high-speed volumetric tomography of human retinal blood flow," *Opt. Express* **17**(5), 4166–4176 (2009).

23. A. S. Singh, T. Schmoll, and R. A. Leitgeb, "Segmentation of Doppler optical coherence tomography signatures using a support-vector machine," *Biomed. Opt. Express* **2**(5), 1328–1339 (2011).

24. S. Makita et al., "Optical coherence angiography," *Opt. Express* **14**(17), 7821–7840 (2006).

25. R. M. Werkmeister et al., "Measurement of absolute blood flow velocity and blood flow in the human retina by dual-beam bidirectional Doppler Fourier-domain optical coherence tomography," *Invest. Ophthalmol. Vis. Sci.* **53**(10), 6062–6071 (2012).

26. A. Szkulmowska et al., "Phase-resolved Doppler optical coherence tomography: limitations and improvements," *Opt. Lett.* **33**(13), 1425–1427 (2008).

27. D. Link et al., "Novel non-contact retina camera for the rat and its application to dynamic retinal vessel analysis," *Biomed. Opt. Express* **2**(11), 3094–3108 (2011).

28. L. Schmetterer and G. Garhofer, "How can blood flow be measured?," *Surv. Ophthalmol.* **52**(Suppl 2), S134–S138 (2007).

29. C. E. Riva et al., "Ocular blood flow assessment using continuous laser Doppler flowmetry," *Acta Ophthalmol.* **88**(6), 622–629 (2010).

30. T. Sugiyama et al., "Use of laser speckle flowgraphy in ocular blood flow research," *Acta Ophthalmol.* **88**(7), 723–729 (2010).

31. Y. Wang et al., "In vivo total retinal blood flow measurement by Fourier domain Doppler optical coherence tomography," *J. Biomed. Opt.* **12**(4), 041215 (2007).

32. S. Makita, T. Fabritius, and Y. Yasuno, "Quantitative retinal-blood flow measurement with three-dimensional vessel geometry determination using ultrahigh-resolution Doppler optical coherence angiography," *Opt. Lett.* **33**(8), 836–838 (2008).

33. B. Baumann et al., "Total retinal blood flow measurement with ultrahigh speed swept source/Fourier domain OCT," *Biomed. Opt. Express* **2**(6), 1539–1552 (2011).

34. C. Blatter et al., "Angle independent flow assessment with bidirectional Doppler optical coherence tomography," *Opt. Lett.* **38**(21), 4433–4436 (2013).

35. V. Doblhoff-Dier et al., "Measurement of the total retinal blood flow using dual beam Fourier-domain Doppler optical coherence tomography with orthogonal detection planes," *Biomed. Opt. Express* **5**(2), 630–642 (2014).

36. T. Schmoll and R. A. Leitgeb, "Heart-beat-phase-coherent Doppler optical coherence tomography for measuring pulsatile ocular blood flow," *J. Biophotonics* **6**(3), 275–282 (2013).

37. V. J. Srinivasan and H. Radhakrishnan, "Total average blood flow and angiography in the rat retina," *J. Biomed. Opt.* **18**(7), 76025 (2013).

38. G. Garhofer et al., "Use of the retinal vessel analyzer in ocular blood flow research," *Acta Ophthalmol.* **88**(7), 717–722 (2010).

39. Y. Li, H. Cheng, and T. Q. Duong, "Blood-flow magnetic resonance imaging of the retina," *NeuroImage* **39**(4), 1744–1751 (2008).

40. A. Tsujikawa et al., "Reproducibility of scanning laser Doppler flowmetry in the rat retina and optic nervehead," *Jpn. J. Ophthalmol.* **44**(3), 257–262 (2000).

41. C. E. Riva, J. E. Grunwald, and S. H. Sinclair, "Laser Doppler velocimetry study of the effect of pure oxygen breathing on retinal blood flow," *Invest. Ophthalmol. Vis. Sci.* **24**(1), 47–51 (1983).

42. B. Kiss et al., "Retinal blood flow during hyperoxia in humans revisited: concerted results using different measurement techniques," *Microvasc. Res.* **64**(1), 75–85 (2002).

43. A. Luksch et al., "Effect of inhalation of different mixtures of O_2 and CO_2 on retinal blood flow," *Br. J. Ophthalmol.* **86**(10), 1143–1147 (2002).

44. E. D. Gilmore et al., "Retinal arteriolar diameter, blood velocity, and blood flow response to an isocapnic hyperoxic provocation," *Am. J. Physiol. Heart Circ. Physiol.* **288**(6), H2912–H2917 (2005).

45. M. Kisilevsky et al., "Concentration-dependent vasoconstrictive effect of hyperoxia on hypercarbia-dilated retinal arterioles," *Microvasc. Res.* **75**(2), 263–268 (2008).

46. R. M. Werkmeister et al., "Response of retinal blood flow to systemic hyperoxia as measured with dual-beam bidirectional Doppler Fourier-domain optical coherence tomography," *PLoS One* **7**(9), e45876 (2012).

47. J. E. Grunwald, J. DuPont, and C. E. Riva, "Retinal haemodynamics in patients with early diabetes mellitus," *Br. J. Ophthalmol.* **80**(4), 327–331 (1996).

48. J. E. Grunwald and S. E. Bursell, "Hemodynamic changes as early markers of diabetic retinopathy," *Curr. Opin. Endocrinol. Diabetes* **3**(4), 98–306 (1996).

49. L. Schmetterer and M. Wolzt, "Ocular blood flow and associated functional deviations in diabetic retinopathy," *Diabetologia* **42**(4), 387–405 (1999).

50. J. Kur, E. A. Newman, and T. Chan-Ling, "Cellular and physiological mechanisms underlying blood flow regulation in the retina and choroid in health and disease," *Prog. Retin. Eye Res.* **31**(5), 377–406 (2012).

51. E. A. Newman, "Functional hyperemia and mechanisms of neurovascular coupling in the retinal vasculature," *J. Cereb. Blood Flow Metab.* **33**(11), 1685–1695 (2013).

52. C. E. Riva, E. Logean, and B. Falsini, "Visually evoked hemodynamical response and assessment of neurovascular coupling in the optic nerve and retina," *Prog. Retin. Eye Res.* **24**(2), 183–215 (2005).

53. A. I. Srienc, Z. L. Kurth-Nelson, and E. A. Newman, "Imaging retinal blood flow with laser speckle flowmetry," *Front. Neuroenergetics* **2**(128), 1–10 (2010).

54. A. Ponticorvo et al., "Laser speckle contrast imaging of blood flow in rat retinas using an endoscope," *J. Biomed. Opt.* **18**(9), 090501 (2013).

55. G. Li et al., "Postocclusive reactive hyperemia occurs in the rat retinal circulation but not in the choroid," *Invest. Ophthalmol. Vis. Sci.* **54**(7), 5123–5131 (2013).

56. A. Mishra and E. A. Newman, "Aminoguanidine reverses the loss of functional hyperemia in a rat model of diabetic retinopathy," *Front. Neuroenergetics* **3**(10), 1–7 (2011).

57. H. Radhakrishnan and V. J. Srinivasan, "Multiparametric optical coherence tomography imaging of the inner retinal hemodynamic response to visual stimulation," *J. Biomed. Opt.* **18**(8), 086010 (2013).

58. G. Garhofer et al., "Diffuse luminance flicker increases blood flow in major retinal arteries and veins," *Vision Res.* **44**(8), 833–838 (2004).

59. M. Lasta et al., "Neurovascular dysfunction precedes neural dysfunction in the retina of patients with type 1 diabetes," *Invest. Ophthalmol. Vis. Sci.* **54**(1), 842–847 (2013).

René M. Werkmeister studied biomedical engineering at the University of Applied Sciences Jena and did his diploma at the Institute de Recherche en Ophthalmologie in Sion, Switzerland, in 2003. In 2003, he joined the research group of Leopold Schmetterer at the Center for Medical Physics and Biomedical Engineering and received his PhD in medical physics in 2010. His research focuses on the development and application of optical methods for biomedical imaging.

Martin Vietauer studied technical physics and received his MSc degree from the Vienna University of Technology. Currently, his PhD research at the Center for Medical Physics and Biomedical Engineering at the Medical University of Vienna covers the field of ocular microcirculation in rodents via Fourier domain Doppler optical coherence tomography (OCT) and fundus imaging using a retinal vessel analyzer (RVA).

Corinna Knopf studied behavior at the University of Graz. After finishing her bachelor's studies she did her master's degree in biomedicine and biotechnology at the University of Veterinary Medicine Vienna. Since October 2012, she has been a PhD-student of the Medical University of Vienna and is working under the supervision of Prof. Leopold Schmetterer in the field of optical coherence tomography on small animal models.

Clemens Fürnsinn studied biology in Vienna. After 7 months of research at the Department of Animal Physiology, Groningen, Netherlands, he elaborated a doctoral thesis at the 1st Medical Department in Vienna and received a PhD in 1990. Thereafter, he held the positions of university assistant, assistant professor and, since 2000, associate professor at the Department of Medicine III in Vienna, interrupted only by a 5-month research visit at the Department of Biochemistry, Oxford, UK.

Rainer A. Leitgeb received his PhD in theoretical physics from the Technical University Vienna, Austria, in 1998, and then joined the

Department of Medical Physics, University of Vienna. From 2004 to 2007, he worked at the EPFL, Switzerland, as project leader. In 2007, he assumed his position as associate professor of medical physics at the Medical University Vienna, specializing in functional and multimodal tomography, and advanced microscopy. In 2014, he was elected fellow of SPIE.

Martin Gröschl received his PhD degree in physics from the Vienna University of Technology (TUW) in 1989. Since 1985, he has been a member of the Sensors and Ultrasonics Group, Institute of Applied Physics, TUW. In 1997, he became associate professor. Since 2008, he has been head of the Sensors and Ultrasonics Group. Recent work covers the development of optical and electronic sensing systems for medical and industrial applications.

Gerhard Garhöfer is a board certified specialist for ophthalmology and associate professor for clinical pharmacology at the Medical University of Vienna, Austria. His main focus of interest includes blood flow regulation in the eye and new pharmacological treatment strategies. He has published more than 100 articles in peer-reviewed journals on these topics.

Leopold Schmetterer received his PhD from the Technical University Vienna in 1989, and thereafter joined the Institute of Medical Physics, Vienna and held a postdoctoral position at the Institute de Recherche en Ophthalmologie in Sion, Switzerland. Currently, he chairs ophthalmic pharmacology at the Department of Clinical Pharmacology and is PI at the Center for Medical Physics and Biomedical Engineering at the Medical University in Vienna. His research interest is directed towards functional imaging of the retina.

Biographies of the other authors are not available.